Chemosphere 346 (2024) 140482

Contents lists available at ScienceDirect

Chemosphere

journal homepage: www.elsevier.com/locate/chemosphere

Measurement of Henry's law constants of ethyl nitrate in deionized water, synthetic sea salt solutions, and *n*-octanol

Kevin D. Easterbrook, Mitchell A. Vona, Hans D. Osthoff *

Department of Chemistry, University of Calgary, 2500 University Drive N.W., Calgary, Alberta, T2N 1N4, Canada

HIGHLIGHTS

- Henry's law constants (H) of ethyl nitrate were measured between 5 °C and 30 °C.
- Values for DI water disagree with the parameterization by Kames and Schurath (1992).
- A salting-out factor of 1.25 ± 0.03 was measured for synthetic sea water.
- H was measured for *n*-octanol; K_{OW}=(10 ± 1) was calculated from $H_{octanol}$ and H_{aq}.
- Ethyl nitrate hydrolysis rates were negligible ($k_l < 1 \times 10^{-4}$ s^{-1}).

GRAPHICAL ABSTRACT

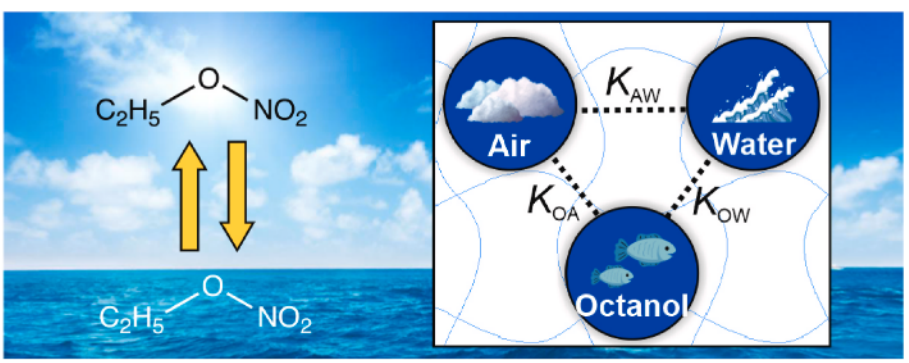

ARTICLE INFO

Handling Editor: R Ebinghaus

Keywords:
Ethyl nitrate
Henry's law constant
Setschenow constant
Octanol-water partition coefficient
Hydrolysis

ABSTRACT

Ethyl nitrate (EN; $C_2H_5ONO_2$) is an important component of atmospheric "odd nitrogen" (NO_y) whose main source is marine emissions. To correctly describe its air-water transfer and model its global distribution, accurate values for its temperature- and salinity-dependent Henry's law solubility constants are needed. Here, we report Henry's law (H_S^{cp}) constants for EN in deionized (DI) water, synthetic sea salt solutions (SSS), and *n*-octanol at temperatures between 278.2 K and 303.2 K. For DI water, H_S^{cp} constants of (2.03 ± 0.06) M atm^{-1} at 293.2 K and (4.88 ± 0.13) M atm^{-1} at 278.2 K were observed (all stated uncertainties are at the 1σ level). The data are best described by $\ln(H_S^{cp}(aq)\ /[M\ atm^{-1}]) = -(16.2 \pm 0.4)+(4.94 \pm 0.11) \times 10^3/T$ and $\ln(H_S^{cp}(octanol)\ /[M\ atm^{-1}]) = -(11.1 \pm 1.9)+(4.15 \pm 0.33) \times 10^3/T$, from which the octanol-water partition coefficient (K_{OW}) was calculated. A temperature-independent salting-out factor of 1.25 ± 0.03 and Setschenow constant of $K_S = (0.33 \pm 0.04)$ mol kg^{-1} were determined for SSS. Liquid-phase losses of EN were negligible in all solvents ($k_l < 1 \times 10^{-4}$ s^{-1}). The $H_S^{cp}(aq)$ values agree with results by Kames (1993) but are between 2% (at 303.2 K) and 19% (at 278.2 K) lower than the widely used parameterization by Kames and Schurath (1992), indicating a systemic bias in the EN literature and modelling of the Earth's nitrogen cycle.

* Corresponding author.
E-mail address: hosthoff@ucalgary.ca (H.D. Osthoff).

https://doi.org/10.1016/j.chemosphere.2023.140482
Received 4 July 2023; Received in revised form 12 October 2023; Accepted 17 October 2023
Available online 22 October 2023

1. Introduction

Short-chain alkyl nitrates (ANs; C_1–C_5 $RONO_2$) are ubiquitous trace gases in the troposphere (Flocke et al., 1991; Roberts et al., 1998; Schneider et al., 1998; Fischer et al., 2000; Russo et al., 2010; Wang et al., 2013; Abeleira et al., 2018). They are often associated with polluted air because they are by-products of the same photochemical oxidation chains involving volatile organic compounds (VOCs) and NO_x (=NO + NO_2) that produce ozone (O_3) (Roberts, 1990). In addition, concentrations of ANs are enhanced in biomass burning plumes (Friedli et al., 2001; Simpson et al., 2002). Further, ANs such as methyl and ethyl nitrate (MN and EN) are emitted directly to the atmosphere from the ocean surface (Atlas, 1988; Chuck et al., 2002; Blake et al., 2003; Dahl et al., 2005; Hughes et al., 2008) and freshwater lakes (Hughes et al., 2010). Fisher et al. (2018) have estimated annual MN and EN global oceanic emissions of 157 and 27 Gg nitrogen per year (Gg N a^{-1}), rates which are of the same order of magnitude as their respective chemical production in the atmosphere.

In the atmosphere, the ANs are considered NO_x reservoir species since they are longer-lived than NO_x with respect to reaction with the hydroxyl radical (OH) (Talukdar et al., 1997) and because they release NO_x back to the atmosphere once oxidized or photo-dissociated. Hence, they often constitute a major fraction of odd nitrogen (NO_y) in remote environments where there are few other sources of nitrogen (Zare et al., 2018; Romer Present et al., 2020) and contribute to the redistribution of nitrogen oxides throughout the troposphere (Atherton, 1989; Fisher et al., 2018). The large nitrogen input from MN and EN oceanic emissions hence accelerates photochemical O_3 and nitrate aerosol production throughout the troposphere.

To correctly describe their air-water transfer (Johnson, 2010) and model the global distributions of ANs, accurate values for their temperature- and salinity-dependent Henry's law solubility constants are needed. Atmospheric chemists typically use Henry solubility in units of M atm^{-1} (H_S^{cp}, for simplicity referred to as H in this manuscript), which is defined as the ratio of liquid phase concentration (in M) over the partial pressure (in atm) of the gas (Sander et al., 2022). In general, the solubility of a gas decreases with increasing salinity; this "salting out" effect is described by the Setschenow (also referred to as Sechenov) equation (Setschenow, 1889):

$$\log\left(\frac{H_{aq}}{H_{salt}}\right) = K_S C_{salt} \quad (1)$$

here, H_{aq} represents the Henry solubility in pure water, H_{salt} represents the Henry solubility in the saline solution whose concentration is given by C_{salt} (~0.7 mol kg^{-1} for seawater (Sarwar et al., 2016)), and K_S is the Setschenow constant.

Compilations of Henry's law data by the National Aeronautics and Space Administration Jet Propulsion Laboratory (NASA-JPL) Panel for Data Evaluation (Burkholder et al., 2020) and by Sander (2023) cite and recommend only the parameterization from a single experimental study, that of Kames and Schurath (1992), who studied the solubility of MN and EN in distilled water and as functions of ionic strength and temperature. This universally used parameterization differs (by ~10% at 293 K, Table 1) from the one in the Ph.D. thesis by Kames (1993). Corroboration of these data is needed to improve the accuracy of chemical transport models and resolve this discrepancy.

Kames and Schurath (1992) measured "salting out" factors $\frac{H_{aq}}{H_{salt}} \approx 1.20 \pm 0.05$ for MN and $\frac{H_{aq}}{H_{salt}} \approx 1.27 \pm 0.05$ for EN in seawater, which are consistent with values predicted by Johnson (2010) of 1.20 for MN and 1.23 for EN. In a footnote, Chuck et al. (2002) reported experimentally determined parameterizations of Henry's law constants for MN and EN in seawater. However, their parameterization yields values that are inconsistent with the data from Kames and Schurath (1992) and have by-and-large been ignored by the community.

The octanol-water partition coefficient (K_{OW}) is a widely used metric to describe the tendency of a molecule to partition from aqueous to organic phases such as lipids, waxes, and natural organic matter (Schwarzenbach et al., 2002; Mackay et al., 2006). To the best of our knowledge, K_{OW} values have not been reported for simple alkyl nitrates such as EN in the open literature. Such data are needed to improve the accuracy of predictions by structure-activity relationships (SAR) for larger organic nitrates.

Our group has recently measured the Henry's law solubility and liquid-phase loss rate (k_l) constants of peroxypropionic nitric anhydride (PPN) in deionized (DI) water and *n*-octanol using a bubble column apparatus coupled to a gas chromatograph (Easterbrook et al., 2023). The PPN samples used in these experiments co-emitted EN, a known by-product of PPN synthesis (Williams et al., 2000), which was baseline-resolved in the chromatograms.

In this work, we measured the H constants for EN for DI water, synthetic sea salt solution (SSS), and *n*-octanol over a range of temperatures pertinent to the sea surface temperature (SST) of the Earth's oceans (Merchant et al., 2019). Our results amend the universally used parameterization by Kames and Schurath (1992). We report Setschenow constants, K_{OW} values, and upper limits to k_l for EN as functions of temperature and discuss implications on the air-water partitioning of EN.

2. Methods

Experimental setup and procedure. The experimental setup has been described by Easterbrook et al. (2023). Briefly, Henry's law solubility constants were measured using a jacketed bubble column apparatus which was temperature-controlled using an external chiller-circulator (Lauda Proline RP 1290). Gas-phase concentrations downstream of the bubble column were monitored by a Varian 3380CP gas chromatograph with electron capture detector (GC-ECD) that had been customized as described by Tokarek et al. (2014). In a typical experiment, the bubble column apparatus was filled with a known volume (V_l) of either DI water (18 MΩ cm^{-1}, Thermo Scientific Barnstead Nanopure Model D11931), SSS, or *n*-octanol (ACS reagent grade, ≥99% purity, used as received). Synthetic sea salt solutions were prepared by dissolving ~17.59 g of

Table 1
Henry's law constants of EN. Errors are at the 1σ level. n/d = not determined.

Solvent	Temperature/Reference	H_S^{cp} (M atm^{-1})						
		303.15 K	298.15 K	293.15 K	289.15 K	285.65 K	281.65 K	278.15 K
DI water	Kames and Schurath (1992)	–	–	2.18	–	–	–	–
DI water	Kames (1993)	–	–	1.91 ± 0.10	–	–	–	–
DI water	Burkholder et al. (2020)[a]	1.2[a]	1.6[a]	2.2[a]	2.8[a]	3.5[a]	4.6[a]	5.7[a]
DI water	This work	1.17 ± 0.01	1.56 ± 0.03	2.03 ± 0.06	2.47 ± 0.11	3.05 ± 0.13	3.98 ± 0.05	4.88 ± 0.13
SSS	This work	0.94 ± 0.01	1.20 ± 0.01	1.67 ± 0.02	1.95 ± 0.03	2.35 ± 0.05	3.22 ± 0.04	4.00 ± 0.06
SSS	Chuck et al. (2002)[b]	0.71	0.9	1.2	1.4	1.7	2.2	2.6
n-octanol	This work	n/d	15.4 ± 1.5	22.2 ± 1.3	24.45 ± 0.92	31.2 ± 2.2	38.8 ± 8.6	41.7 ± 1.4

[a] Values recommended by the NASA-JPL evaluation panel with an uncertainty factor of 2–10.
[b] The equation provided by Chuck et al. (2002), ln() = -4137//T/ + 10.78, gives unreasonable values and appears to be in error. In Table S4, values were calculated from -ln() = -4137//T/ + 10.78, with /T/ in kelvin, from which the values in Table 1 were calculated using Eq. (3).

"Instant Ocean"® sea salt in 500 mL of DI water (Richards and Finlayson-Pitts, 2012). Once the desired temperature was achieved (after ~20 min), gas streams containing EN in nitrogen (N_2; delivered from the blow-off of a liquid N_2 dewar) were generated using a diffusion source containing an aliquot of PPN in tridecane solution which had been synthesized as described by Mielke and Osthoff (2012). This solution co-emitted EN, a known by-product of PPN synthesis (Williams et al., 2000). The gas stream containing EN was bubbled through the liquid in the bubble column for ~5 min at a flow rate of ~25 standard (0 °C, 1 bar) cubic centimeters per minute (sccm). The incoming gas stream was then briefly (~30 s) backflushed with N_2 delivered via a calibrated mass flow controller (MFC, MKS Instruments) and then exhausted to a waste line. For experiments in DI water and SSS, the N_2 was humidified using a second DI water bubbler placed between the MFC and the main bubble column apparatus to minimize solvent loss via evaporation. The EN concentration ($c_{g,t}$) was then monitored as a function of time (t) by the GC-ECD. Sample chromatograms are shown in Fig. 2 of Easterbrook et al. (2023). The experiment was repeated, systematically varying the ratio of (volumetric) flow rate to liquid volume ($\frac{\Phi}{V_l}$) as summarized in Tables S1–S3 in the supporting information (S.I.) section.

Calculation methods. The concentration of EN decays due to a combination of first-order loss and gas-liquid equilibration, i.e., partitioning of EN from the liquid reservoir to the gas stream. Kames and Schurath (1995) showed that under these conditions the analyte's gas-phase concentration (and hence the peak area observed by the GC) decreases according to the following relationship:

$$\ln\left(\frac{c_{g,0}}{c_{g,t}}\right) = \left(\frac{\Phi}{H_S^{cc} \times V_l} + k_l\right)t \quad (2)$$

Here, k_l is the liquid-phase loss rate constant of EN, and H_S^{cc} is the dimensionless Henry solubility (Sander et al., 2022), related to H by:

$$H = H_S^{cp} = \frac{H_S^{cc}}{RT} \quad (3)$$

where T is the temperature in kelvin, and R is the universal gas constant (~0.08205 L atm mol^{-1} K^{-1}).

Since the chromatographic peak areas (A) are proportional to c_g (Tokarek et al., 2014), linear regression plots of $\ln\left(\frac{A_0}{A_t}\right)$ $\left(= \ln\left(\frac{c_{g,0}}{c_{g,t}}\right)\right)$ as a function of (volumetric) flow rate to liquid volume ratio, ($\frac{\Phi}{V_l}$), yield a slope of $1/H_S^{cc}$ and an intercept of k_l. For each experiment, the peak areas were determined using a macro in Igor Pro (Wavemetrics Inc.) as described by Tokarek et al. (2014) that fits parameters of a Gaussian expression to the observed peaks.

The temperature dependence of H can be described using a Van't Hoff-type equation, i.e.,

$$\ln(H) = A_H - \frac{B_H}{T} + C_H \ln(T) \approx A_H - \frac{B_H}{T} \quad (4)$$

where A_H, B_H, and C_H are simple curve fitting parameters, with A_H and B_H proportional to the entropy and enthalpy of solvation, respectively (Staudinger and Roberts, 2001). Over limited temperature ranges, H can often be well represented by a linear relationship, and the C_H term is omitted (Burkholder et al., 2020). Equation (4) was used to parameterize the H constants for EN in DI water, SSS, and *n*-octanol. From these data, K_{OW} was calculated using:

$$K_{OW} = \frac{H_S^{cp}(\text{octanol})}{H_S^{cp}(\text{aq})} \quad (5)$$

3. Results

Representative plots of $\ln\left(\frac{c_{g,0}}{c_{g,t}}\right)$ as a function of t are shown in Fig. 1. In this example, EN was observed downstream from 100.0 mL of SSS at a temperature of 16.00 °C. Plots such as those shown in Fig. 1 were linear with Pearson correlation coefficients (r) > 0.994 for all experiments.

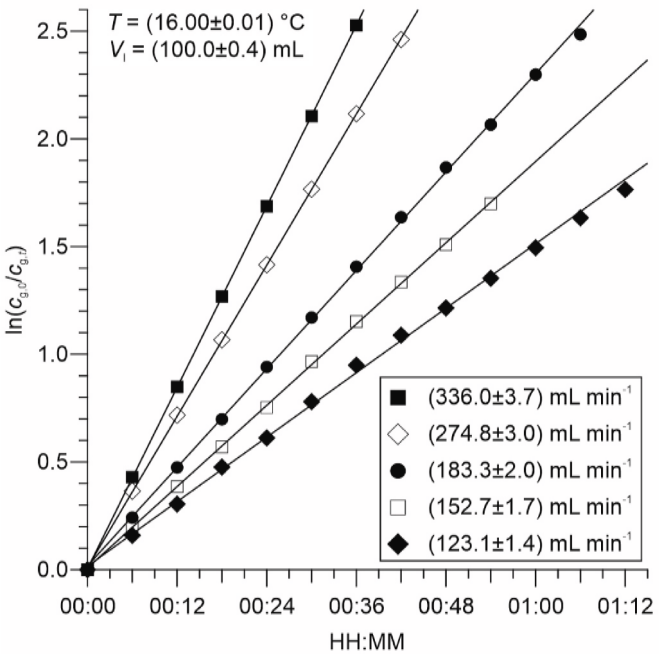

Fig. 1. Example plots of ln ($c_{g,0}/c_{g,t}$) versus t for five different volumetric flow rates. Here, EN was observed downstream from 100.0 mL of synthetic sea salt solutions at a temperature of 16.00 °C. The straight lines are linear fits to the data at each temperature.

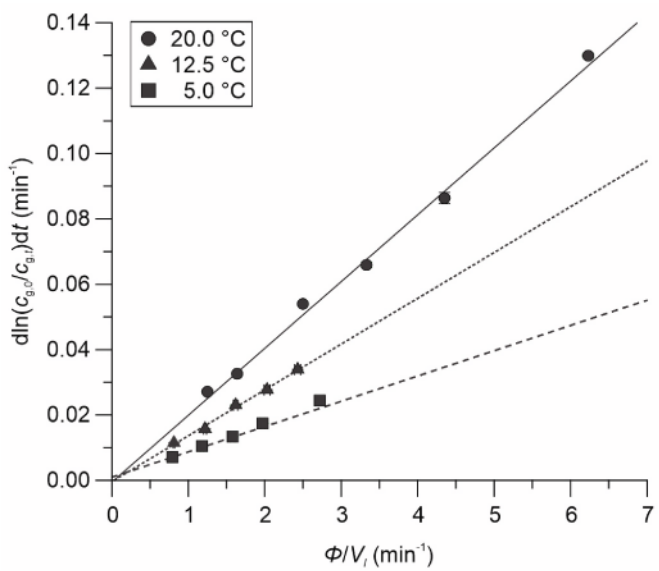

Fig. 2. Plots of dln ($c_{g,0}/c_{g,t}$)/dt versus Φ/V_l in deionized water at 20.0 °C (●), 12.5 °C (▲) and 5.0 °C (■). Error bars are 1σ precision. The straight lines are linear fits to the data at each temperature.

Sample plots of $\frac{d}{dt}\ln\left(\frac{c_{g,0}}{c_{g,t}}\right)$ versus $\left(\frac{\Phi}{V_l}\right)$ at temperatures of 20.0 °C, 12.5 °C and 5.0 °C for experiments with DI water are shown in Fig. 2. Linear regression analyses of plots such as those shown in Fig. 2 yields slopes equal to $1/H_S^{cc}$ (Table S4), from which H was calculated using Eq. (3). The results are summarized in Table 1, alongside literature values.

The equation provided by Chuck et al. (2002), $\ln(H_S^{cc}) = -4137/T + 10.78$, gives unreasonable values and appears to be in error. In Table S4, H_S^{cc} values were calculated from -ln (H_S^{cc}) = −4137/T + 10.78, with T in

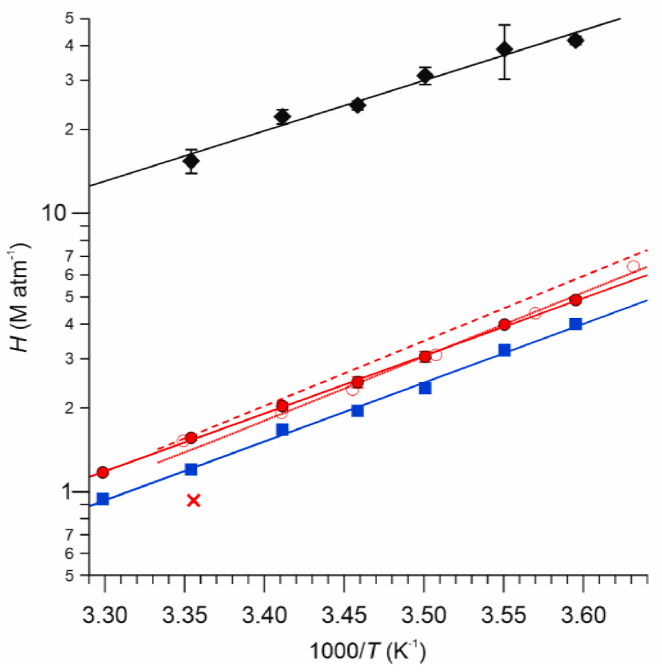

Fig. 3. Henry's law constants for EN in DI water (●, red colour), in synthetic seawater (■, blue colour), and in *n*-octanol (◆, black colour) as functions of temperature. Fits to the data are shown as solid lines. Data from Figure 4 of Kames and Schurath (1992) in DI water were extracted using "Engauge Digitizer" software and are shown as open circles (○, red colour). The GROMHE estimate (Raventos-Duran et al., 2010) for DI water at 298 K is shown as a cross (× , red colour). The narrowly dotted line (···, red colour) is the fit from the Ph. D. thesis of Kames (1993) for DI water, whereas the widely dashed line (--, red colour) is the fit reported by Kames and Schurath (1992). (For interpretation of the references to colour in this figure legend, the reader is referred to the Web version of this article.)

kelvin, from which the values in Table 1 were calculated using Eq. (3).

Fig. 3 summarizes the H constants measured in this work in the form of Van't Hoff plots. Our data for DI water are shown as solid circles in red colour and are consistent with the data by Kames and Schurath (1992), reproduced in Fig. 3 as open circles. Our data are also consistent with the parameterization in the Ph.D. thesis of Kames (1993), shown as a narrowly dotted line, but are inconsistent with the parameterization by Kames and Schurath (1992), shown as a widely dashed line; the latter parameterization is currently recommended by the NASA-JPL panel (Burkholder et al., 2020).

Fits to the full version of Eq. (4) of the data shown in Fig. 3 yields C_H terms whose ±1σ uncertainty encompasses zero (data not shown); the C_H term was thus omitted in subsequent fits. The resulting values of A_H and B_H are summarized in Table 2, along with literature values. A combined fit of our data with those of Kames and Schurath (1992) for DI water yields $\ln(H_S^{cp}(aq)/[M\ atm^{-1}]) = -(16.2 \pm 0.4) + (4.94 \pm 0.11) \times 10^3/T$.

The Henry's law solubility constants of EN in SSS are smaller than those in DI water (Fig. 3 and Table 1) by a temperature-independent factor of 1.25 ± 0.03 (average ± 1σ) (Table 3). Setschenow constants were calculated by rearrangement of Eq. (1) and using a salt concentration of seawater of 0.69 mol kg^{-1} (Sarwar et al., 2016); the resulting K_S values are 0.33 ± 0.04 on average (Table 3).

Measured H constants in *n*-octanol are larger than those in DI water and SSS (Fig. 3) and ranged from (41.7 ± 1.4) M atm^{-1} at 278 K to (15.4 ± 1.5) M atm^{-1} at 298 K (Table 1). The data are best described by $\ln(H_S^{cp}(octanol)/[M\ atm^{-1}]) = -(11.1 \pm 1.9) + (4.15 \pm 0.33) \times 10^3/T$ (Table 2).

n-Octanol - water partition coefficients of EN, calculated using Eq. (2), are summarized in Table 4. The calculated K_{OW} values exhibit no temperature dependence between 5.0 °C and 25.0 °C, with a minimum value of 8.6 ± 0.4 at 5.0 °C, a maximum value of 11.0 ± 0.7 at 20.0 °C (Table 4).

The liquid-phase loss rate constants were determined from the intercepts of plots such as those shown in Fig. 2 and are summarized in Table S5. In general, k_l values are small in all solvents ($<10^{-4}\ s^{-1}$ at the 95% confidence level). The largest values were observed for DI water at 25 °C and 30 °C, $\sim 5 \times 10^{-5}\ s^{-1}$. In most cases, the ±2σ confidence interval of k_l encompasses zero, indicating that EN hydrolysis was negligible on the time scale of these experiments.

4. Discussion

Henry's law solubility constants for n-octanol and determination of K_{OW} In this work, H constants in DI water were measured for EN at temperatures between 5 °C and 30 °C. This constitutes only the second determination of H for EN in DI water to date. Our measurements are consistent with the raw data by Kames and Schurath (1992) and the parameterization in the doctoral thesis by Kames (1993), but not with the parameterization given in the journal article by Kames and Schurath (1992) on which the current recommendation by the NASA-JPL panel (Burkholder et al., 2020) is based. Our results differ from the currently recommended parameterization by between 2% (at 30 °C) and 19% (at 5 °C). The incorrect parameterization by Kames and Schurath (1992) has been used extensively in the literature to model EN abundances in the Earth system, not only in the context of its partitioning between the troposphere and the ocean or lake surfaces (Chuck et al., 2002; Dahl et al., 2005; Hughes et al., 2010; Russo et al., 2010; Neuman et al., 2012; Fisher et al., 2018) but also in the context of its foliar uptake (Lockwood et al., 2008; Place et al., 2022). Our data suggest that all studies that relied on the incorrect Henry's law parameterization are biased.

Henry's law solubility constants for SSS. The "salting out" factor observed in this work of 1.25 ± 0.03 is consistent with the salting out factor of 1.27 ± 0.05 measured by Kames and Schurath (1992) for an authentic North Sea water sample and the value of 1.23 estimated by Johnson (2010). On the other hand, the H constants of EN in SSS observed in this work are (40 ± 8)% larger than the values calculated from the parameterization by Chuck et al. (2002) for reasons that are unclear. Considering the lack of experimental details provided by Chuck et al. (2002) and the excellent agreement of our data with the data by Kames and Schurath (1992) and Kames (1993), we are confident in the accuracy of our results.

Henry's law solubility constants for *n*-octanol and determination of K_{OW}. To the best of our knowledge, this work constitutes the first experimental determination of $H_S^{cp}(octanol)$ and K_{OW} for EN to date (Baskaran et al., 2021). The K_{OW} values observed in this work (Table 4) are small, which suggests that EN will neither significantly partition to the organic aerosol phase nor bioaccumulate in animal fatty tissue.

Utility of experimental data to SAR models. Numerous SAR models have been developed for estimating Henry's law and octanol-water partition constants of atmospheric organics such the GROup contribution Method for Henry's law Estimate (GROMHE) (Raventos-Duran et al., 2010) or the United States Environmental Protection Agency's EPISuite™ (2023). Our experimentally determined H value in DI water at 25 °C is a factor of 1.7 × larger than the (GROMHE) estimate (Fig. 3), and our empirically derived K_{OW} value of 10 ± 1 is a factor of 1.8 × smaller than the value of ~18 calculated using the EPISuite™ (Chemspider, 2023). While this is encouraging, it highlights the need for experimental work to help constrain and refine predictive models. Recently, Wang et al. (2017) have called for more experimental data to help refine predictions of gas-aqueous phase and gas–organic phase partitioning coefficients for the myriad of molecules that contribute to the ambient aerosol phase and whose properties can only be determined by SAR models.

Table 2
Temperature dependence of Henry's law constants of EN, derived by linear fitting of Eq. (4) with $C_H = 0$ to the data shown in Fig. 3. Uncertainties are at the 1σ level. n/d = not disclosed. N/A = not applicable.

Solvent	Reference	r^2 (%)	$-B_H$ (10^3 K^{-1})	A_H (unitless)	$-R \times B_H = -\Delta H^0_{sol}$ (kJ mol^{-1})	$R \times A_H$ (J K^{-1} mol^{-1})
water	Kames and Schurath (1992)	n/d	5.35 ± 0.18	−17.5 ± 0.6	44.53 ± 1.5	−145.5 ± 5.0
water	Kames (1993)	n/d	5.29 ± 0.18	−17.4 ± 0.6	44 ± 1.5	−144.7 ± 5.0
water	Burkholder et al. (2020)[a]	N/A	5.36	−17.5	44.6	−145
DI water	This work	99.83	4.85 ± 0.12	−15.9 ± 0.4	40.4 ± 1.0	−131.9 ± 3.4
DI water	This work[b]	99.24	4.94 ± 0.11	−16.2 ± 0.4	41.1 ± 0.9	−134.5 ± 3.3
SSS	This work	99.57	4.85 ± 0.14	−16.1 ± 0.5	40.3 ± 1.2	−133.5 ± 4.1
SSS	Chuck et al. (2002)	n/d	4.43	−15.0	36.8	−124.3
n-octanol	This work	97.58	4.15 ± 0.33	−11.1 ± 1.9	34.5 ± 2.7	−92.4 ± 15.7

[a] Literature compilation with an uncertainty factor of 2–10.
[b] Data from this work combined with those of Kames and Schurath (1992).

Table 3
Setschenow constants of EN for seawater. Errors are at the 1σ level. The salt concentration of SSS was assumed to be equal to 0.69 mol kg^{-1}.

T (K)	$H^{cc}_{S,aq}$	$H^{cc}_{S,SSS}$	$\frac{H^{cc}_{S,aq}}{H^{cc}_{S,SSS}}$	K_S (kg mol^{-1})
278.15	111 ± 3	91.3 ± 1.4	1.22 ± 0.04	0.29 ± 0.02
281.65	91.9 ± 1.1	74.5 ± 1.0	1.23 ± 0.02	0.30 ± 0.01
285.65	71.5 ± 3.1	55.0 ± 1.1	1.30 ± 0.06	0.38 ± 0.03
289.15	58.5 ± 2.6	46.3 ± 0.7	1.26 ± 0.06	0.33 ± 0.03
293.15	48.8 ± 1.5	40.2 ± 0.5	1.22 ± 0.04	0.28 ± 0.02
298.15	38.0 ± 0.7	29.4 ± 0.2	1.29 ± 0.03	0.37 ± 0.01
303.15	29.1 ± 0.2	23.4 ± 0.3	1.24 ± 0.02	0.31 ± 0.01
Average			1.25 ± 0.03	0.33 ± 0.04

Table 4
n-Octanol - water partition coefficients of EN. Errors are at the 1σ level.

Temperature	298.15 K	293.15 K	289.15 K	285.65 K	281.65 K	278.15 K
K_{OW}	9.9 ± 1.0	11.0 ± 0.7	9.9 ± 0.6	10.2 ± 0.8	9.7 ± 2.2	8.6 ± 0.4

Constraints on hydrolysis rates. The hydrolysis of AN has been an active research area for many decades (Baker and Easty, 1950). Several recent studies have invoked hydrolysis following aerosol uptake as a loss pathway of isoprene or terpene nitrates (e.g., (Liu et al., 2012; Rindelaub et al., 2015; Vasquez et al., 2020; Morales et al., 2021),), sparking renewed interest in the mechanism of AN hydrolysis (Keshavarz et al., 2021), which corroborated the existence of both acid- and base-catalyzed hydrolysis pathways. More recently, hydrolysis following leaf stomatal uptake has been proposed for a simple AN (i.e., isopropyl nitrate) (Place et al., 2022).

Our results indicate that liquid-phase hydrolysis rates of EN are slow, with rate coefficients of $\sim 5 \times 10^{-5}$ s^{-1} in DI water at 25 °C. However, because EN does not hydrolyze to a significant extent on the time scale of our experiments, our method is not ideal to make reliable measurements of small k_l values. Hu et al. (2011) measured an acid-catalyzed rate constant of 1.1×10^{-4} s^{-1} in D_2SO_4 solution, whereas our k_l measurements were in deionized and unbuffered solutions in the pH neutral regime (i.e., mildly acidic due to atmospheric CO_2) under conditions where the hydrolysis rate is likely slower (Keshavarz et al., 2021). Thus, the value of k_l at intermediate pH values is uncertain, and measurements of EN hydrolysis kinetics as a function of pH using a static method (similar to the study by Hu et al. (2011)) are needed.

5. Conclusions

The Henry's law constants of EN in DI water, SSS, and *n*-octanol were measured between 278.15 K and 303.15 K using a jacketed bubble column apparatus. For DI water, the observed values are smaller than calculated using the parameterization by Kames and Schurath (1992), which is currently recommended by the NASA-JPL panel. Chemical transport models relying on their incorrect parameterization are systematically biased and should be updated. Setschenow constants calculated based on data in this paper are consistent with previous measurements by Kames and Schurath (1992) and a numerical prediction by Johnson (2010). Compilations of K_{OW} values are currently lacking experimental data of simple alkyl nitrates. In this work, K_{OW} of EN was determined experimentally for the first time, partially addressing this knowledge gap.

Author contributions

KDE (EN with SSS and *n*-octanol) and MAV (EN with DI water) carried out the experiments and reduced the data. HDO conceptualized the experiments. KDE and HDO drafted and edited the manuscript.

Declaration of competing interest

The authors declare that they have no known competing financial interests or personal relationships that could have appeared to influence the work reported in this paper.

Data availability

Data will be made available on request.

Acknowledgments

This work was made possible by the financial support of the Natural Sciences and Engineering Research Council of Canada (NSERC) in the form of a Discovery grant to HDO (RGPIN/03849–2016). The authors thank Dr. Jost Kames for confirming an error in the values tabulated by Kames and Schurath (1992) and for sharing excerpts of his Ph.D. thesis work (Kames, 1993). KDE acknowledges an NSERC undergraduate student research award (USRA).

Appendix A. Supplementary data

Supplementary data to this article can be found online at https://doi.org/10.1016/j.chemosphere.2023.140482.

References

Abeleira, A., Sive, B., Swarthout, R.F., Fischer, E.V., Zhou, Y., Farmer, D.K., 2018. Seasonality, sources and sinks of C-1-C-5 alkyl nitrates in the Colorado Front Range. Elementa-Science of the Anthropocene 6, 45. https://doi.org/10.1525/elementa.299.

Atherton, C.S., 1989. Organic nitrates in remote marine environments: evidence for long range transport. Geophys. Res. Lett. 16, 1289–1292. https://doi.org/10.1029/GL016i011p01289.

Atlas, E., 1988. Evidence for C3-alkyl nitrates in rural and remote atmospheres. Nature 331, 426–428. https://doi.org/10.1038/331426a0.

Baker, J.W., Easty, D.M., 1950. Hydrolysis of organic nitrates. Nature 166. https://doi.org/10.1038/166156a0, 156-156.
Baskaran, S., Lei, Y.D., Wania, F., 2021. A database of experimentally derived and estimated octanol–air partition ratios (KOA). J. Phys. Chem. Ref. Data 50, 043101. https://doi.org/10.1063/5.0059652.
Blake, N.J., Blake, D.R., Swanson, A.L., Atlas, E., Flocke, F., Rowland, F.S., 2003. Latitudinal, vertical, and seasonal variations of C1-C4 alkyl nitrates in the troposphere over the Pacific Ocean during PEM-Tropics A and B: oceanic and continental sources. J. Geophys. Res. Atmos. 108, 8242. https://doi.org/10.1029/2001JD001444.
Burkholder, J.B., Sander, S.P., Abbatt, J.P.D., Barker, J.R., Cappa, C., Crounse, J.D., Dibble, T.S., Huie, R.E., Kolb, C.E., Kurylo, M.J., Orkin, V.L., Percival, C.J., Wilmouth, D.M., Wine, P.H., 2020. Chemical Kinetics and Photochemical Data for Use in Atmospheric Studies, Evaluation Number 19. National Aeronautics and Space Administration, Jet Propulsion Laboratory, California Institute of Technology, Pasadena, California.
Chemspider, Royal Society of Chemistry, http://www.chemspider.com/Chemical-Structure.11756.html (accessed June 27, 2023).
Chuck, A.L., Turner, S.M., Liss, P.S., 2002. Direct evidence for a marine source of C-1 and C-2 alkyl nitrates. Science 297, 1151–1154. https://doi.org/10.1126/science.1073896.
Dahl, E.E., Yvon-Lewis, S.A., Saltzman, E.S., 2005. Saturation anomalies of alkyl nitrates in the tropical Pacific Ocean. Geophys. Res. Lett. 32, L20817 https://doi.org/10.1029/2005gl023896.
Easterbrook, K.D., Vona, M.A., Nayebi-Astaneh, K., Miller, A.M., Osthoff, H.D., 2023. Measurement of Henry's law and liquid-phase loss rate constants of peroxypropionic nitric anhydride (PPN) in deionized water and in n-octanol. Atmos. Chem. Phys. 23, 311–322. https://doi.org/10.5194/acp-23-311-2023.
Fischer, R.G., Kastler, J., Ballschmiter, K., 2000. Levels and pattern of alkyl nitrates, multifunctional alkyl nitrates, and halocarbons in the air over the Atlantic Ocean. J. Geophys. Res. 105, 14473–14494. https://doi.org/10.1029/1999JD900780.
Fisher, J.A., Atlas, E.L., Barletta, B., Meinardi, S., Blake, D.R., Thompson, C.R., Ryerson, T.B., Peischl, J., Tzompa-Sosa, Z.A., Murray, L.T., 2018. Methyl, ethyl, and propyl nitrates: global distribution and impacts on reactive nitrogen in remote marine environments. J. Geophys. Res. Atmos. 123, 12429–12451. https://doi.org/10.1029/2018jd029046.
Flocke, F.M., Volz-Thomas, A., Kley, D., 1991. Measurements of alkyl nitrates in rural and polluted air masses. Atmos. Environ. A 25, 1951–1960. https://doi.org/10.1016/0960-1686(91)90276-D.
Friedli, H.R., Atlas, E., Stroud, V.R., Giovanni, L., Campos, T., Radke, L.F., 2001. Volatile organic trace gases emitted from North American wildfires. Global Biogeochem. Cycles 15, 435–452. https://doi.org/10.1029/2000gb001328.
Hu, K.S., Darer, A.I., Elrod, M.J., 2011. Thermodynamics and kinetics of the hydrolysis of atmospherically relevant organonitrates and organosulfates. Atmos. Chem. Phys. 11, 8307–8320. https://doi.org/10.5194/acp-11-8307-2011.
Hughes, C., Chuck, A.L., Turner, S.M., Liss, P.S., 2008. Methyl and ethyl nitrate saturation anomalies in the Southern Ocean (3665S, 3070W). Environ. Chem. 5, 11–15. https://doi.org/10.1071/EN07083.
Hughes, C., Kettle, A.J., Unazi, G.A., Weston, K., Jones, M.R., Johnson, M.T., 2010. Seasonal variations in the concentrations of methyl and ethyl nitrate in a shallow freshwater lake. Limnol. Oceanogr. 55, 305–314. https://doi.org/10.4319/lo.2010.55.1.0305.
Johnson, M.T., 2010. A numerical scheme to calculate temperature and salinity dependent air-water transfer velocities for any gas. Ocean Sci. 6, 913–932. https://doi.org/10.5194/os-6-913-2010.
Kames, J., 1993. Henry-Koeffizienten und Hydrolysekonstanten organischer Nitrate in der Atmosphare: Physikochemische Parameter zur Beschreibung heterogener Verlustprozesse. Universitat, Bonn.
Kames, J., Schurath, U., 1992. Alkyl nitrates and bifunctional nitrates of atmospheric interest - Henry Law Constants and their temperature dependencies. J. Atmos. Chem. 15, 79–95. https://doi.org/10.1007/BF00053611.
Kames, J., Schurath, U., 1995. Henry's law and hydrolysis rate constants for peroxyacyl nitrates (PANs) using a homogeneous gas-phase source. J. Atmos. Chem. 21, 151–164. https://doi.org/10.1007/BF00696578.
Keshavarz, F., Thornton, J.A., Vehkamaki, H., Kurten, T., 2021. Reaction mechanisms underlying unfunctionalized alkyl nitrate hydrolysis in aqueous aerosols. ACS Earth Space Chem. 5, 210–225. https://doi.org/10.1021/acsearthspacechem.0c00253.
Liu, S., Shilling, J.E., Song, C., Hiranuma, N., Zaveri, R.A., Russell, L.M., 2012. Hydrolysis of organonitrate functional groups in aerosol particles. Aerosol Sci. Technol. 46, 1359–1369. https://doi.org/10.1080/02786826.2012.716175.
Lockwood, A.L., Filley, T.R., Rhodes, D., Shepson, P.B., 2008. Foliar uptake of atmospheric organic nitrates. Geophys. Res. Lett. 35, L15809 https://doi.org/10.1029/2008GL034714.
Mackay, D., Shiu, W.Y., Ma, K.-C., Lee, S.C., 2006. Handbook of Physical-Chemical Properties and Environmental Fate for Organic Chemicals, second ed. CRC/Taylor & Francis, Boca Raton, FL.
Merchant, C.J., Minnett, P.J., Beggs, H., Corlett, G.K., Gentemann, C., Harris, A.R., Hoyer, J., Maturi, E., 2019. 2 - global sea surface temperature. In: Hulley, G.C., Ghent, D. (Eds.), Taking the Temperature of the Earth. Elsevier, pp. 5–55.
Mielke, L.H., Osthoff, H.D., 2012. On quantitative measurements of peroxycarboxylic nitric anhydride mixing ratios by thermal dissociation chemical ionization mass spectrometry. Int. J. Mass Spectrom. 310, 1–9. https://doi.org/10.1016/j.ijms.2011.10.005.
Morales, A.C., Jayarathne, T., Slade, J.H., Laskin, A., Shepson, P.B., 2021. The production and hydrolysis of organic nitrates from OH radical oxidation of β-ocimene. Atmos. Chem. Phys. 21, 129–145. https://doi.org/10.5194/acp-21-129-2021.
Neuman, J.A., Aikin, K.C., Atlas, E.L., Blake, D.R., Holloway, J.S., Meinardi, S., Nowak, J. B., Parrish, D.D., Peischl, J., Perring, A.E., Pollack, I.B., Roberts, J.M., Ryerson, T.B., Trainer, M., 2012. Ozone and alkyl nitrate formation from the Deepwater Horizon oil spill atmospheric emissions. J. Geophys. Res. 117, D09305 https://doi.org/10.1029/2011jd017150.
Place, B.K., Delaria, E.R., Cohen, R.C., 2022. Leaf stomatal uptake of alkyl nitrates. Environ. Sci. Technol. Lett. 9, 186–190. https://doi.org/10.1021/acs.estlett.1c00793.
Raventos-Duran, T., Camredon, M., Valorso, R., Mouchel-Vallon, C., Aumont, B., 2010. Structure-activity relationships to estimate the effective Henry's law constants of organics of atmospheric interest. Atmos. Chem. Phys. 10, 7643–7654. https://doi.org/10.5194/acp-10-7643-2010.
Richards, N.K., Finlayson-Pitts, B.J., 2012. Production of gas phase NO_2 and halogens from the photochemical oxidation of aqueous mixtures of sea salt and nitrate ions at room temperature. Environ. Sci. Technol. 46, 10447–10454. https://doi.org/10.1021/es300607c.
Rindelaub, J.D., McAvey, K.M., Shepson, P.B., 2015. The photochemical production of organic nitrates from α-pinene and loss via acid-dependent particle phase hydrolysis. Atmos. Environ. 100, 193–201. https://doi.org/10.1016/j.atmosenv.2014.11.010.
Roberts, J.M., 1990. The atmospheric chemistry of organic nitrates. Atmos. Environ. A 24, 243–287. https://doi.org/10.1016/0960-1686(90)90108-Y.
Roberts, J.M., Bertman, S.B., Parrish, D.D., Fehsenfeld, F.C., Jobson, B.T., Niki, H., 1998. Measurement of alkyl nitrates at chebogue point, nova scotia during the 1993 North atlantic regional experiment (NARE) intensive. J. Geophys. Res. Atmos. 103, 13569–13580. https://doi.org/10.1029/98jd00266.
Romer Present, P.S., Zare, A., Cohen, R.C., 2020. The changing role of organic nitrates in the removal and transport of NO_x. Atmos. Chem. Phys. 20, 267–279. https://doi.org/10.5194/acp-20-267-2020.
Russo, R.S., Zhou, Y., Haase, K.B., Wingenter, O.W., Frinak, E.K., Mao, H., Talbot, R.W., Sive, B.C., 2010. Temporal variability, sources, and sinks of C1-C5 alkyl nitrates in coastal New England. Atmos. Chem. Phys. 10, 1865–1883. https://doi.org/10.5194/acp-10-1865-2010.
Sander, R., 2023. Compilation of Henry's law constants (version 5.0.0) for water as solvent. Atmos. Chem. Phys. 23, 10901–12440. https://doi.org/10.5194/acp-23-10901-2023.
Sander, R., Acree, W.E., De Visscher, A., Schwartz, S.E., Wallington, T.J., 2022. Henry's law constants (IUPAC Recommendations 2021). Pure Appl. Chem. 94, 71–85. https://doi.org/10.1515/pac-2020-0302.
Sarwar, G., Kang, D.W., Foley, K., Schwede, D., Gantt, B., Mathur, R., 2016. Technical note: examining ozone deposition over seawater. Atmos. Environ. 141, 255–262. https://doi.org/10.1016/j.atmosenv.2016.06.072.
Schneider, M., Luxenhofer, O., Deissler, A., Ballschmiter, K., 1998. C1-C15 alkyl nitrates, benzyl nitrate, and bifunctional nitrates: measurements in California and South Atlantic air and global comparison using C_2Cl_4 and $CHBr_3$ as marker molecules. Environ. Sci. Technol. 32, 3055–3062. https://doi.org/10.1021/es980132g.
Schwarzenbach, R.P., Gschwend, P.M., Imboden, D.M., 2002. Organic liquid–water partitioning. In: Environmental Organic Chemistry. Wiley, Hoboken, New Jersey, USA, pp. 213–244.
Setschenow, J., 1889. Über die Konstitution der Salzlösungen auf Grund ihres Verhaltens zu Kohlensäure. Z. Phys. Chem. 4U, 117–125. https://doi.org/10.1515/zpch-1889-0409.
Simpson, I.J., Meinardi, S., Blake, D.R., Blake, N.J., Rowland, F.S., Atlas, E., Flocke, F., 2002. A biomass burning source of C-1-C-4 alkyl nitrates. Geophys. Res. Lett. 29, 2168. https://doi.org/10.1029/2002GL016290.
Staudinger, J., Roberts, P.V., 2001. A critical compilation of Henry's law constant temperature dependence relations for organic compounds in dilute aqueous solutions. Chemosphere 44, 561–576. https://doi.org/10.1016/S0045-6535(00)00505-1.
Talukdar, R.K., Herndon, S.C., Burkholder, J.B., Roberts, J.M., Ravishankara, A.R., 1997. Atmospheric fate of several alkyl nitrates. 1. Rate coefficients of the reactions alkyl nitrates with isotopically labelled hydroxyl radicals. J. Chem. Soc. Faraday. Trans. 93, 2787–2796. https://doi.org/10.1039/A701780D.
Tokarek, T.W., Huo, J.A., Odame-Ankrah, C.A., Hammoud, D., Taha, Y.M., Osthoff, H.D., 2014. A gas chromatograph for quantification of peroxycarboxylic nitric anhydrides calibrated by thermal dissociation cavity ring-down spectroscopy. Atmos. Meas. Tech. 7, 3263–3283. https://doi.org/10.5194/amt-7-3263-2014.
Vasquez, K.T., Crounse, J.D., Schulze, B.C., Bates, K.H., Teng, A.P., Xu, L., Allen, H.M., Wennberg, P.O., 2020. Rapid hydrolysis of tertiary isoprene nitrate efficiently removes NO_x from the atmosphere. Proc. Natl. Acad. Sci. USA 117, 33011–33016. https://doi.org/10.1073/pnas.2017442117.
Wang, M., Shao, M., Chen, W., Lu, S., Wang, C., Huang, D., Yuan, B., Zeng, L., Zhao, Y., 2013. Measurements of C1–C4 alkyl nitrates and their relationships with carbonyl

compounds and O_3 in Chinese cities. Atmos. Environ. 81, 389–398. https://doi.org/10.1016/j.atmosenv.2013.08.065.

Wang, C., Yuan, T., Wood, S.A., Goss, K.U., Li, J., Ying, Q., Wania, F., 2017. Uncertain Henry's law constants compromise equilibrium partitioning calculations of atmospheric oxidation products. Atmos. Chem. Phys. 17, 7529–7540. https://doi.org/10.5194/acp-17-7529-2017.

Williams, J., Roberts, J.M., Bertman, S.B., Stroud, C.A., Fehsenfeld, F.C., Baumann, K., Buhr, M.P., Knapp, K., Murphy, P.C., Nowick, M., Williams, E.J., 2000. A method for the airborne measurement of PAN, PPN, and MPAN. J. Geophys. Res. 105, 28943–28960. https://doi.org/10.1029/2000JD900373.

Zare, A., Romer, P.S., Nguyen, T., Keutsch, F.N., Skog, K., Cohen, R.C., 2018. A comprehensive organic nitrate chemistry: insights into the lifetime of atmospheric organic nitrates. Atmos. Chem. Phys. 18, 15419–15436. https://doi.org/10.5194/acp-18-15419-2018.

Update

Chemosphere
Volume 348, Issue , January 2024, Page

DOI: https://doi.org/10.1016/j.chemosphere.2023.140777

Chemosphere 348 (2024) 140777

Contents lists available at ScienceDirect

Chemosphere

journal homepage: www.elsevier.com/locate/chemosphere

Corrigendum

Corrigendum to "Measurement of Henry's law constants of ethyl nitrate in deionized water, synthetic sea salt solutions, and *n*-octanol" [Chemosphere **346** (2024) 140482]

Kevin D. Easterbrook, Mitchell A. Vona, Hans D. Osthoff *

Department of Chemistry, University of Calgary, 2500 University Drive N.W., Calgary, Alberta, T2N 1N4, Canada

The authors regret to inform you that there were typographical errors in a line of Table 2 tabulating the temperature dependence of Henry's law constants of EN measured by our group.

The authors would like to thank Dr. Rolf Sander for alerting us to this error and apologise for any inconvenience caused.

The correct content should read as follows.

Solvent	Reference	r^2 (%)	$-B_H$ (10^3 K^{-1})	A_H (unitless)	$-R \times B_H = -\Delta H_{sol}$ (kJ mol^{-1})	$R \times A_H$ (J K^{-1} mol^{-1})
DI water	This work	99.83	4.79 ± 0.06	−15.6 ± 0.4	39.8 ± 0.5	−130.0 ± 3.4

DOI of original article: https://doi.org/10.1016/j.chemosphere.2023.140482.

* Corresponding author.
E-mail address: hosthoff@ucalgary.ca (H.D. Osthoff).

https://doi.org/10.1016/j.chemosphere.2023.140777

Available online 27 November 2023